diversity

MDPI

Article

Effects of Ocean Currents in the Western Pacific Ocean on Net-Phytoplankton Community Compositions

Zhuo Chen [1], Jun Sun [2,*], Dawei Chen [3], Shihao Wang [3,4], Hao Yu [3,4], Hongtao Chen [5] and Min Wang [6]

1 College of Biotechnology, Tianjin University of Science and Technology, Tianjin 300457, China; chenzhuo981@163.com
2 College of Marine Science and Technology, China University of Geosciences, Wuhan 430074, China
3 Research Centre for Indian Ocean Ecosystem, Tianjin University of Science and Technology, Tianjin 300457, China; chendawei0914@163.com (D.C.); shihao223@126.com (S.W.); haha653@gmail.com (H.Y.)
4 Institute of Marine Science and Technology, Shandong University, Qingdao 266200, China
5 Key Laboratory of Marine Chemistry Theory and Technology, Ministry of Education, Ocean University of China, Qingdao 266100, China; chenht@ouc.edu.cn
6 College of Marine Life Science, Ocean University of China, Qingdao 266003, China; mingwang@ouc.edu.cn
* Correspondence: phytoplankton@163.com

Abstract: Phytoplankton are known as important harbingers of climate change in aquatic ecosystems. This study investigated phytoplankton community structure in the western Pacific Ocean (WPO) in 2017 and revealed the spatial variability of phytoplankton in community composition and abundance, as well as their relationship to physical processes and environmental factors. The phytoplankton community was mainly composed of Dinophyta (221), followed by Bacillariophyta (105), Cyanophyta (4), and Chrysophyta (2). The cyanobacteria *Trichodesmium* were the dominants throughout the study period. Correlation analysis showed that dinoflagellates were mainly affected by temperature, while diatoms were significantly correlated with nutrients (silicate, phosphate, nitrite, nitrate). Phytoplankton was divided into five groups by cluster analysis, and the distribution of different groups was related to circulation and hydrological characteristics. In contrast, the highest abundance of diatoms and dinoflagellates was found in the New Guinea Coastal Current (NGCC) region, while the highest abundance of cyanobacteria was found in the Northern Equatorial Counter Current (NECC) region. Overall, we found that not only temperature and salinity, but also ocean currents and nutrients, influence the distribution of phytoplankton communities in the WPO.

Keywords: phytoplankton; community structure; western Pacific Ocean; ocean currents; environmental factors; nutrients

Citation: Chen, Z.; Sun, J.; Chen, D.; Wang, S.; Yu, H.; Chen, H.; Wang, M. Effects of Ocean Currents in the Western Pacific Ocean on Net-Phytoplankton Community Compositions. *Diversity* **2021**, *13*, 428. https://doi.org/10.3390/d13090428

Academic Editor: Bert W. Hoeksema

Received: 20 August 2021
Accepted: 3 September 2021
Published: 5 September 2021

1. Introduction

As the most important producers in marine ecosystems, phytoplankton not only absorb carbon dioxide and regulate global climate change, but also provide energy through photosynthesis [1]. Phytoplankton communities play an important role in biogeochemical cycles and pelagic food webs, and they also support the energy needs of marine ecosystems [2]. They are widely distributed in the upper layer, and the distribution of phytoplankton species and their community structure are usually associated with the dominant marine environment (unique nutrient structure) [3]. The distribution of phytoplankton in seawater is usually strongly influenced by ocean circulation and mesoscale hydrographic features [4]. Some specific currents and water masses are inhabited by specific native species, a property that can be used to indicate water movement [5]. For this reason, the distribution of many phytoplankton species is closely related to unique environmental factors in many marine ecosystems.

The Pacific Ocean covers about a third of the earth and nearly half of the sea surface around the world. The boundaries of the tropical western Pacific Ocean (WPO) are very irregular, with numerous islands and complex ocean currents. Specifically, there are three dominant current systems in the region: the North Equatorial Current (NEC, 10°–25° N), the Northern Equatorial Counter Current (NECC) (4°–10° N), and the South Equatorial Current (SEC, 4° N–20° S) [6]. In addition, there are the New Guinea Coastal Current (NGCC) and the New Guinea Coastal Undercurrent (NGCU) on the coast of New Guinea. Owing to the high solar radiation throughout the year and the influence of the equatorial currents flowing, warm water accumulates in the western equatorial Pacific Ocean, forming the largest warm water region called the western Pacific warm pool (WPWP), with a thermocline thickness of 100–150 m, which was 3–6 °C higher than the eastern equatorial Pacific Ocean [7,8].

The study of phytoplankton in the Kuroshio region of the WPO dates to the 1970s, and a lot of work has been done by domestic and foreign scholars. The distribution and composition of plankton in the Kuroshio area were reported in detail by Kawarada et al. [9]. Shiro Fujioka [10] analyzed the Kuroshio water masses near the Sea of Japan and used phytoplankton as indicator species. In 1997, Sun [11] and Liu [12] further investigated the composition and abundance distribution of planktonic diatoms and dinoflagellates in the Ryukyu Islands and nearby waters. Chen [13] and Chen [14] proposed that the abundance of *Trichodesmium* was higher in the Kuroshio area due to the deeper nitrate thermocline and the lower nitrate concentration in the surface layer. The density of *Trichodesmium* in the Kuroshio region was very high. The available data need to be improved and updated. Although some quantitative assessments of the phytoplankton community structure of WPO have been obtained in previous studies, information on the influence of circulation on the phytoplankton composition in the region is lacking. Therefore, analyzing the distribution of the WPO phytoplankton community and the effects of species composition and circulation will provide indispensable information for future studies. In this study, the community structure of phytoplankton in the whole water column was explored by characterizing the community structure of net-phytoplankton in the investigated sea area. The relationships between phytoplankton and environmental factors and their responses to the effects of circulation were analyzed. Thus, certain information can be accumulated for the ecological study of phytoplankton in the region.

2. Material and Method

The cruise was carried out from 142–163° E and 1–40° N in the WPO onboard R/V "*Dongfanghong* 2", covering 63 stations from October 6th to December 7th in 2017. As shown in Figure 1, the survey area was divided into two sections: Section A (stations assigned to the longitude of 143–146° E) and Section B (stations assigned along the equator). These stations were sampled between 0 and 200 m depth by vertical tows with the plankton net (mouth opening 0.25 m^2, mesh size 20 μm). Samples were fixed in 5% buffered formalin and stored in the dark. In the laboratory, phytoplankton samples are observed under a microscope (AE2000, Motic, Xiamen, China) [15]. Phytoplankton identification was conducted as described by Jin [16], Isamu Y [17], and Sun [18]. Species identification was as close as possible to the species level.

Seawater samples were collected by a SeaBird CTD (SBE 9/11 plus) equipped with Go-Flo bottles, and temperature and salinity were recorded at the same time. The temperature and salinity of the water column were calculated by means of a trapezoidal integration of the different levels of seawater temperature and salinity. Nutrient samples from different layers were placed in PE bottles and stored at −20 °C for laboratory nutrient analysis [19]. Nitrate, nitrite, ammonium, phosphate, and silicate were also analyzed on board by spectrometric methods [20]. Chlorophyll *a* (chl *a*) samples were filtered through Whatman GF/F filters (0.7 μm) for seawater samples (1 L) and subsequently saved under –20 °C. Chl *a* was extracted in laboratory without light by 90% acetone, and then Turner fluorimeter (model 10-AU) was used to measure the chl *a* concentration [21]. The sampling layers were 5 m, 30 m, 75 m, 100 m, 150 m, and 200 m.

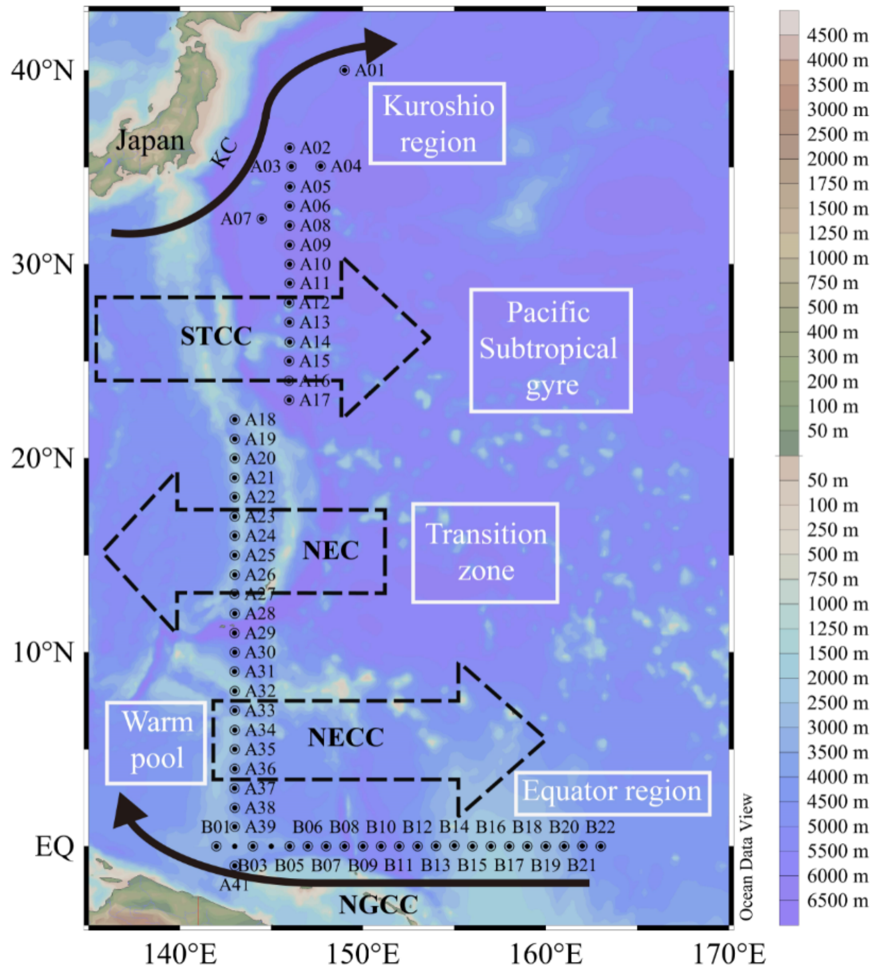

Figure 1. Study area and locations of the sampling stations in the WPO. Map of the WPO shows the major geographic names and the surface currents, including the Kuroshio Current (KC), the Subtropical Counter Current (STCC), the North Equatorial Current (NEC), the Northern Equatorial Counter Current (NECC), and the New Guinea Coastal Current (NGCC) [22,23].

Dominance index (Y) was calculated to describe the species dominance in the phytoplankton community. The calculation equation was as follows:

$$Y = \frac{n_i}{N} f_i \tag{1}$$

where n_i is the number of the individual species, N is the total number of all species, and f_i is the occurrence frequency of the species in a sample.

The abundance of phytoplankton cells in water column was calculated through the trapezoidal integral method [24]:

$$\mathrm{P} = \left\{ \sum_{i=1}^{n-1} \frac{\mathrm{P}_{i+1} + \mathrm{P}_i}{2} (\mathrm{D}_{i+1} - \mathrm{D}_i) \right\} / (\mathrm{D}_n - \mathrm{D}_1) \tag{2}$$

where P is the average value of phytoplankton abundance in water column, Pi is the abundance value of phytoplankton in layer i, i + 1 is the layer i + 1, D_n is the maximum sampling depth, D_i is the depth of layer i, and n is the sampling level.

Horizontal and depth-integrated distribution of phytoplankton and physiochemical parameters were projected using Ocean Data View 4.7.6 and ArcGIS 10.8. The histogram was plotted with Origin (Version 8.5). Pearson correlation and canonical correspondence analysis (CCA) between assemblages and physicochemical parameters were performed using the R package vegan (version 2.5–7) [25] to explain the relationship between the environmental parameters (temperature, salinity, and nutrients) and phytoplankton community structure.

3. Result

3.1. Phytoplankton Species Composition

Phytoplankton samples from the WPO were analyzed, and 332 species belonging to 68 genera in 4 phyla were identified, including Bacillariophyta, Dinophyta, Cyanophyta, and Chrysophyta. There were 105 diatoms belonging to 37 genera (31.63% of total species), 221 species in 28 genera of dinoflagellates (66.57%), 4 cyanobacteria species, and 2 chrysophyceae species (Table 1). The distribution of phytoplankton (Figure 2a) is mainly determined by *Cyanobacteria*. The distribution of dinoflagellate (Figure 2b) shows that most of the sites of dinoflagellate are evenly distributed, and diatom is more dominant in some stations near the shore. *Trichodesmium thiebautii* is the main species of *Trichodesmium* and is abundantly distributed in the surveyed sea area (Figure 2c). The abundance of *Trichodesmium* reaches the maximum value (12.905×10^3 cells m^{-3}) at the A35 station of the investigated sea area. The distribution of dominant species (Figure 2d) shows that there is a rich diversity of phytoplankton in the investigated sea area. The dominant species of dinoflagellate in this survey is *Ceratium kofoidii*, and the maximum value appears at A28 station (5.619×10^3 cells m^{-3}). *Planktoniella foromsa* is the dominant species of diatom in this survey, and the maximum value appears at B19 station (13.276×10^3 cells m^{-3}). *Thalassiothrix longissima* is a common species of Kuroshio, which is dominant at A01 and A02 stations, and reaches the peak at B18 station with higher diatom abundance (Table 2). Cluster analysis was used to analyze the similarity of phytoplankton taxa. The results of the cluster analysis were used to analyze the similarity between phytoplankton taxa based on their abundance during the 2017 cruise. The cluster analysis revealed five distinct phytoplankton communities (Figure 3). Phytoplankton groups containing fewer than four stations were not considered as significant clusters. Clusters were assigned different color symbols and plotted in the sampling area (Figure 3).

Table 1. The numbers of phytoplankton species and genera in the WPO.

Phylum	Genera	Species	Ratio of Richness (%)
Bacillariophyta	37	105	31.63
Dinophyta	28	221	66.57
Cyanophyta	2	4	1.20
Chrysophyta	1	2	0.60

Table 2. Dominant phytoplankton species in the WPO.

Species	Percentage (%)	Frequency (*fi*)	Dominance (*Y*)	Maximum (10^3 Cells m^{-3})	Average (10^3 Cells m^{-3})	Maximum Stations
T. thiebautii	65.67	0.952	0.6254	8895.529	374.425	A35
Trichodesmium erythraeum	19.46	0.889	0.1730	2128.430	110.979	A36
Trichodesmium hildebrandtii	12.07	0.746	0.0900	2782.329	68.807	A35
C. kofoidii	0.18	0.952	0.0017	5.619	1.037	A28
Prorocentrum leniculatum	0.15	1.000	0.0015	3.300	0.845	A36
Richelia intracellularis	0.14	0.698	0.0010	7.947	0.805	A24
P. foromsa	0.12	0.794	0.0010	13.276	0.688	B19
Coscinodiscus marginato-lineatus	0.10	0.968	0.0009	2.844	0.542	B18
Thalassiosira subtilis	0.09	0.968	0.0009	3.433	0.512	B07
Prorocentrum compressum	0.08	1.000	0.0007	1.836	0.425	B07
T. longissima	0.08	0.937	0.0007	6.542	0.445	B18
Thalassiosira minima	0.07	1.000	0.0007	2.540	0.415	B19

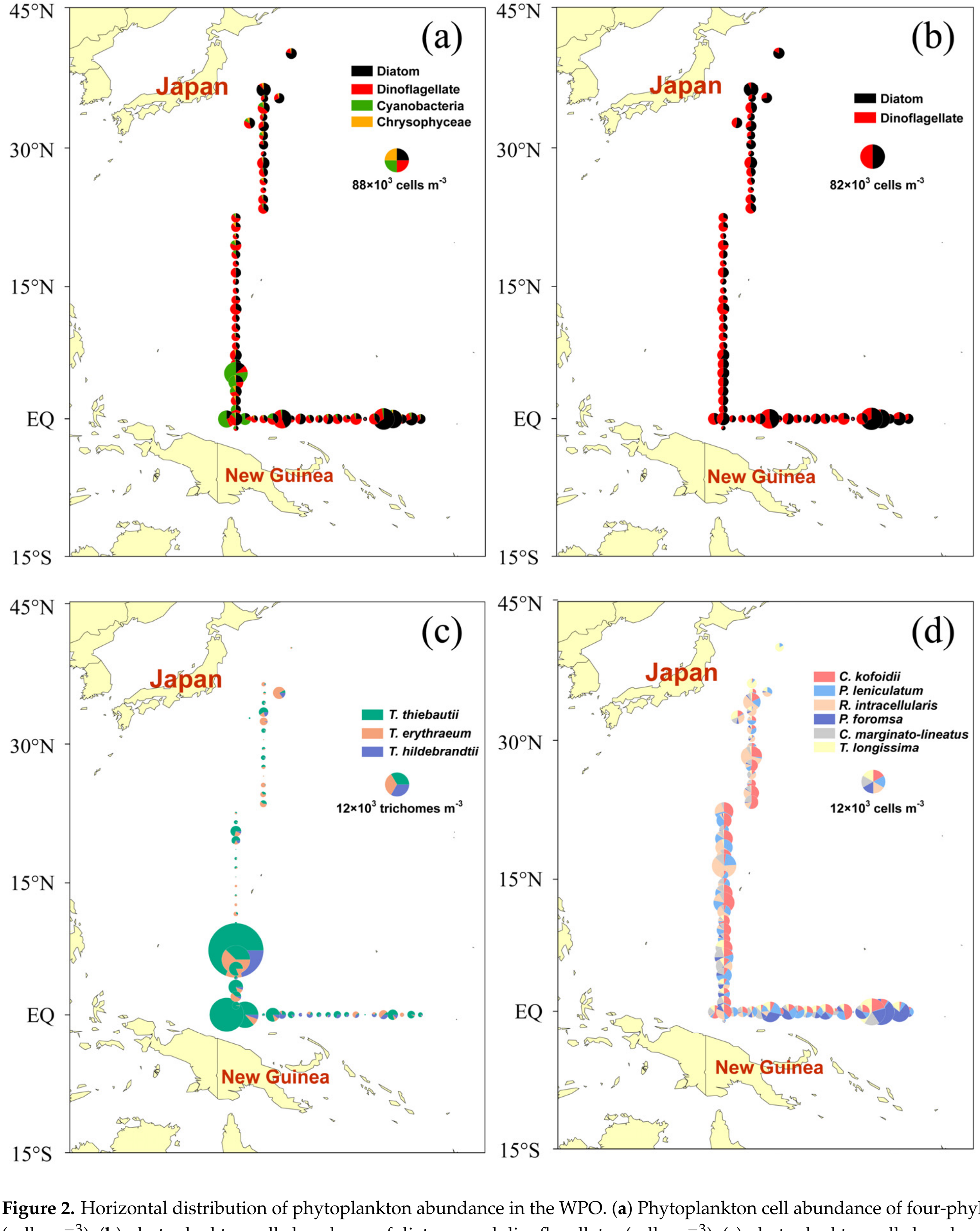

Figure 2. Horizontal distribution of phytoplankton abundance in the WPO. (**a**) Phytoplankton cell abundance of four-phyla (cells m^{-3}); (**b**) phytoplankton cell abundance of diatoms and dinoflagellates (cells m^{-3}); (**c**) phytoplankton cell abundance of *Trichodesmium* (trichomes m^{-3}); (**d**) dominant species abundance (cells m^{-3}).

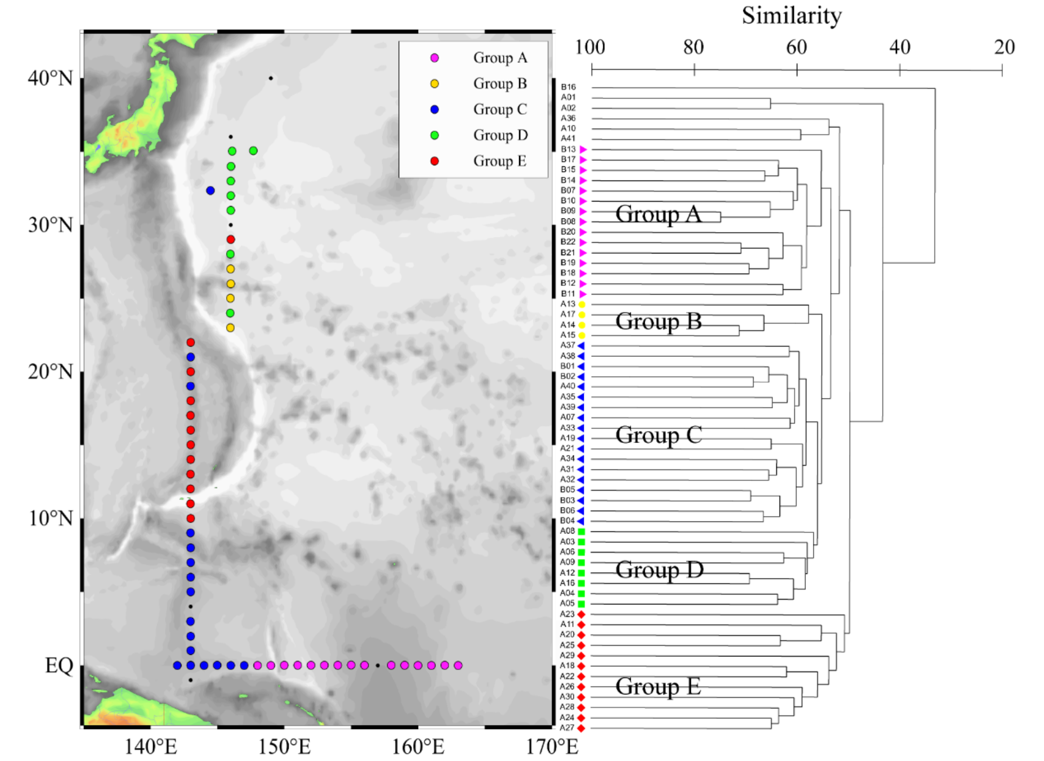

Figure 3. Location of the different phytoplankton groups in the WPO.

3.2. Environmental Characteristics of the Survey Area

Phytoplankton clustering analysis divided the 63 stations surveyed into five groups (Figure 3). The different groups had different hydrological characteristics. These hydrological characteristics included temperature (T), salinity (S), chl *a*, silicate (SiO_3^{2-}), phosphate (PO_4^{3-}), nitrate (NO_3^-), nitrite (NO_2^-), and ammonium (NH_4^+). We found that the five groups had different characteristics. Group A had the highest mean temperature, the highest mean salinity, the highest mean nutrient concentration, and a deeper mixed layer with a thickness of about 125 m; Group B had the shallowest mixed layer with a thickness of about 30 m; Group C had the highest mean silicate concentration; Group D had the lowest mean temperature and the lowest mean salinity; and Group E had moderate mean temperature, salinity, and nutrient levels (Table 3, Figure 4).

Table 3. Average (± standard deviations) values for nutrients (μmol L^{-1}), temperature (°C), salinity, and chlorophyll a (μg L^{-1}) for each phytoplankton community group identified by the cluster analysis in the WPO.

	Group A	Group B	Group C	Group D	Group E
PO_4^{3-}	0.37 ± 0.07	0.13 ± 0.08	0.27 ± 0.10	0.16 ± 0.06	0.13 ± 0.05
NO_2^-	0.23 ± 0.12	0.05 ± 0.01	0.12 ± 0.04	0.06 ± 0.01	0.09 ± 0.02
NO_3^-	2.66 ± 0.87	0.70 ± 0.52	2.15 ± 1.07	2.06 ± 0.79	0.66 ± 0.47
NH_4^+	0.87 ± 0.21	1.32 ± 0.43	1.51 ± 0.56	0.86 ± 0.09	1.49 ± 0.62
SiO_3^{2-}	1.83 ± 0.29	2.00 ± 0.17	2.23 ± 1.07	2.62 ± 0.60	1.57 ± 0.45
temperature	28.24 ± 0.45	23.50 ± 0.46	27.29 ± 1.49	22.72 ± 1.08	26.89 ± 1.48
salinity	35.06 ± 0.18	34.98 ± 0.11	34.54 ± 0.24	34.80 ± 0.08	34.62 ± 0.31
chl *a*	0.41 ± 0.11	0.27 ± 0.46	0.34 ± 0.08	0.31 ± 0.08	0.27 ± 0.08

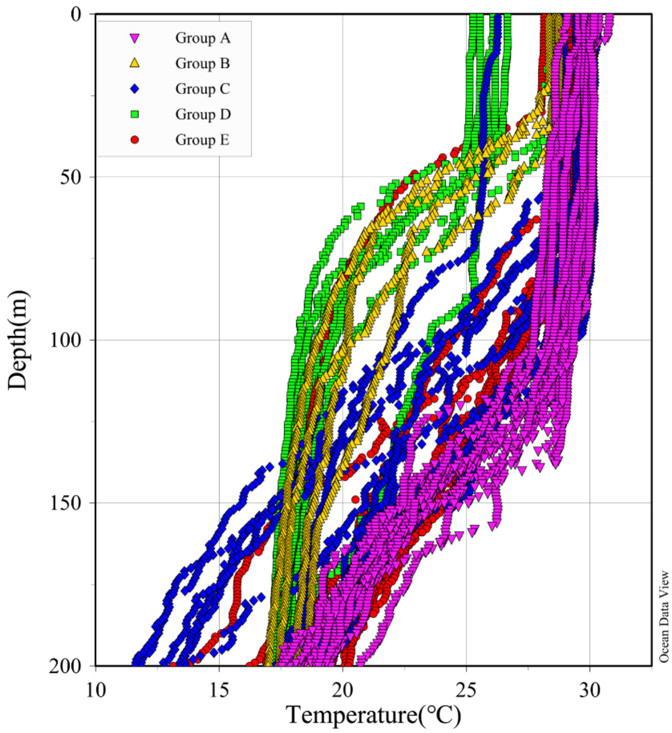

Figure 4. The temperature profiles of the upper 200 m at the survey stations to distinguish the five groups (Group A–E).

3.3. Phytoplankton Community Structure of Five Groups

Cluster analysis showed that phytoplankton communities have a spatial distribution structure in the currents of the WPO. In the five groups, the phytoplankton had different proportions of cell abundance. The cell abundance of the four-phyla phytoplankton also differed in the five groups (Figure 5). The dominant species of phytoplankton had different mean cell abundance in the five groups (Table 4). Overall, the highest abundance of diatoms and dinoflagellates was in Group A, and the highest abundance of cyanobacteria in Group C.

Table 4. List of phytoplankton community group characteristics (average ± standard deviations) identified by cluster analysis in the WPO.

	Group A	Group B	Group C	Group D	Group E
Phytoplankton	211,796 ± 129,387	91,379 ± 60,250	1,454,796 ± 3,127,957	175,003 ± 211,356	77,120 ± 101,440
Diatoms	12,176 ± 12,454	4188 ± 2124	6664 ± 3171	8109 ± 2944	4022 ± 1794
Dinoflagellates	9820 ± 7323	6136 ± 2530	7306 ± 2106	5748 ± 3264	5834 ± 3357
Cyanobacteria	189,548 ± 114,153	80,735 ± 55,865	1,440,161 ± 3,126,653	160,503 ± 210,271	67,168 ± 100,680
Chrysophyceae	252 ± 268	321 ± 496	665 ± 560	643 ± 361	96 ± 157
T. thiebautii	96,835 ± 102,200	44,784 ± 34,253	1,093,840 ± 2,302,347	23,845 ± 21,450	37,684 ± 64,710
T. erythraeum	37,156 ± 53,088	33,982 ± 41,793	162,062 ± 292,659	119,011 ± 173,439	23,111 ± 35,473
T. hildebrandtii	55,556 ± 49,123	1486 ± 2972	183,590 ± 649,917	15,922 ± 33,384	4509 ± 14,216
C. kofoidii	965 ± 908	1312 ± 830	1251 ± 921	918 ± 1059	1261 ± 1652
P. leniculatum	782 ± 629	177 ± 190	867 ± 612	495 ± 371	1443 ± 993
R. intracellularis	0 ± 0	483 ± 278	669 ± 690	1725 ± 2011	1865 ± 2174
P. foromsa	2389 ± 3473	55 ± 52	334 ± 261	83 ± 58	9 ± 16
C. marginato-lineatus	632 ± 812	545 ± 318	719 ± 583	259 ± 255	519 ± 434
T. subtilis	705 ± 978	473 ± 223	598 ± 498	536 ± 685	199 ± 163
P. compressum	524 ± 448	373 ± 388	482 ± 403	266 ± 183	428 ± 353
T. longissima	988 ± 1594	64 ± 63	388 ± 377	230 ± 110	65 ± 99
T. minima	583 ± 679	413 ± 309	403 ± 426	513 ± 306	300 ± 209

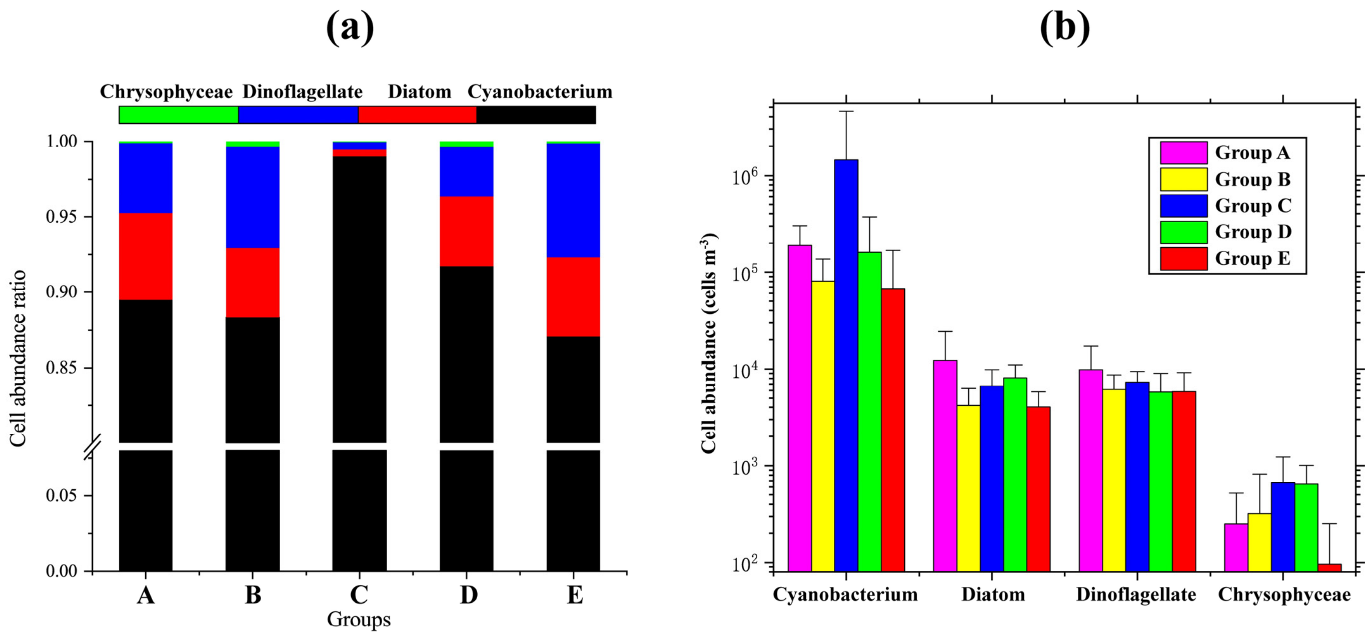

Figure 5. Species composition and changes between groups of phytoplankton in the WPO. (**a**) The cell abundance ratio of the four-phyla phytoplankton in each group; (**b**) The cell abundance (cells m^{-3}) of the four-phyla phytoplankton in each group.

Group A was distributed along the equator and mainly affected by the NGCC. The total phytoplankton abundance in Group A was not the highest (2.12 × 10^{5} cells m^{-3}) among the five phytoplankton groups, but the abundance of diatoms and dinoflagellates in Group A was the highest (1.22 × 10^{4} cells m^{-3} and 0.98 × 10^{4} cells m^{-3}). Cyanobacteria, diatoms, dinoflagellates, and chrysophyceaes accounted for 89.49%, 5.75%, 4.64%, and 0.12% of the total phytoplankton, respectively. The abundance of *P. foromsa* (2.39 × 10^{3} cells m^{-3}) and *T. longissima* (9.88 × 10^{2} cells m^{-3}) was higher than other groups. Additionally, *R. intracellularis* was not found in Group A.

Group B contained sites affected by the STCC. *P. leniculatum* of Group B had the lowest abundance (1.77 × 10^{2} cells m^{-3}). Cyanobacteria accounted for 88.35%, diatoms 4.58%, dinoflagellates 6.72%, and chrysophyceaes 0.35% of the total phytoplankton. *C. kofoidii* had the highest abundance (1.31 × 10^{3} cells m^{-3}) in Group B among the five groups.

Group C was mainly affected by the NECC. Group C had the highest abundance of total phytoplankton (1.45 × 10^{6} cells m^{-3}). Group C of phytoplankton was mainly composed of cyanobacteria; cyanobacteria accounted for 98.99% of the total phytoplankton, diatoms accounted for 0.46% of the total phytoplankton, dinoflagellates accounted for 0.50% of the total phytoplankton, and chrysophyceaes accounted for 0.05% of the total phytoplankton. *C. marginato-lineatus* had the highest abundance (7.19 × 10^{2} cells m^{-3}) among the five groups in Group C.

Group D mainly contained stations affected by the STCC and KC. Cyanobacteria, diatoms, dinoflagellates and chrysophyceaes accounted for 91.71%, 4.63%, 3.29% and 0.37% of the total phytoplankton respectively. *Fragilariopsis doliolus* had the highest abundance (6.78 × 10^{2} cells m^{-3}) in Group D among the five groups.

Group E, located in the middle of the sampling area, was mainly affected by the NEC. Group E was the group with the lowest total phytoplankton abundance (7.71 × 10^{4} cells m^{-3}), and the abundance (4.51 × 10^{3} cells m^{-3}, 0.01 × 10^{3} cells m^{-3}, 0.07 × 10^{3} cells m^{-3}) of *T. hildebrandtii*, *P. foromsa*, and *T. longissima* in this group was also very low. Cyanobacteria, diatoms, dinoflagellates and chrysophyceaes accounted for 87.10%, 5.21%, 7.56%, and 0.13% of the total phytoplankton, respectively.

3.4. Phytoplankton Distribution in Relation to Environmental Factors

The influence of environmental factors on the phytoplankton community structure in the WPO was assessed using Pearson′s correlation (Figure 6) and CCA analysis (Figure 7). The phytoplankton community in the region was significantly influenced by environmental factors. Phytoplankton cell abundance was extremely significantly correlated with cyanobacteria ($p < 0.001$), indicating that cyanobacteria are the main component of phytoplankton in this survey area. Diatom was extremely significantly correlated with phosphate and nitrate ($p < 0.01$) and was also significantly correlated with silicate and nitrite ($p < 0.05$). This shows that the abundance of diatom is more affected by nutrients. There was a significant correlation between dinoflagellate and temperature ($p < 0.05$), and temperature plays an important role in the growth of dinoflagellate. Different dominant species had different responses to the aquatic environment. The abundance of *T. erythraeum*, *P. compressum*, *C. marginato-linetus*, and *P. Leniculatum* were positively correlated with nitrates and silicates concentration. The abundance of *P. foromsa*, *T. hildebrandtii* were positively correlated with phosphate and nitrite concentration.

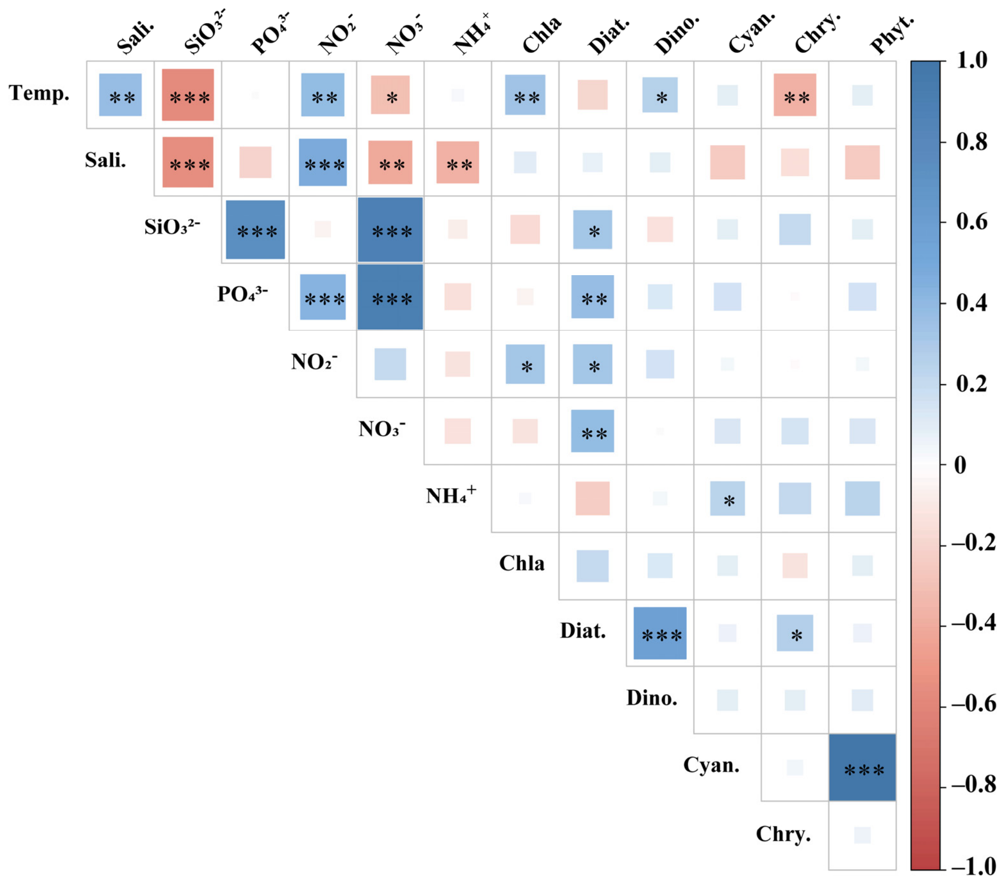

Figure 6. Pearson′s correlation between phytoplankton and environmental factors. Samples number: $n = 63$, * For $p < 0.05$, ** for $p < 0.01$, *** for $p < 0.001$. Temp.: temperature; Sali.: salinity; Diat.: Diatom; Dino.: Dinoflagellate; Cyan.: Cyanobacteria; Chry.: Chrysophyceae; NO_3^-: nitrate; NO_2^-: nitrite, NH_4^+: ammonium, PO_4^{3-}: phosphate, and SiO_3^{2-}: silicate.

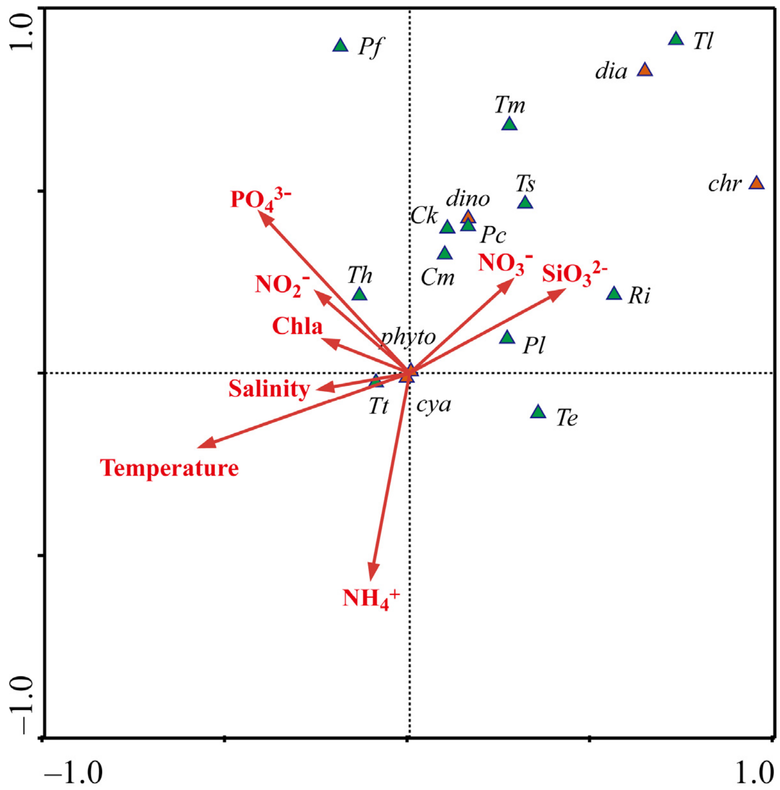

Figure 7. Canonical Correlation Analysis of the dominant phytoplankton species and environmental factors in the surface layer in the WPO during autumn, 2017. dia: diatoms; dino: dinoflagellates; cya: cyanobacteria; chr: chrysophyceae; Tt: *Trichodesmium thiebautii*; Te: *Trichodesmium erythraeum*; Th: *Trichodesmium hildebrandtii*; Ck: *Ceratium kofoidii*; Pl: *Prorocentrum leniculatum*; Ri: *Richelia intracellularis*; Pf: *Planktoniella foromsa*; Cm: *Coscinodiscus marginato-lineatus*; Ts: *Thalassiosira subtilis*; Pc: *Prorocentrum compressum*; Tl: *Thalassiothrix longissima*; Tm: *Thalassiosira minima*.

4. Discussion

4.1. Hydrological Conditions and Corresponding Phytoplankton Community Structure

The study spanned five different hydrological characteristics distributed across the 40° N to equatorial cross-section, Kuroshio region, subtropical gyre, transitional zone, warm pool, and equator region [26–29]. The difference in salinity between the surface water in the transition zone and the Subsurface Chlorophyll Maximum (SCM) confirms the existence of positive precipitation budget phenomenon in this area [30]. However, at higher resolution, neither phytoplankton species richness nor species distribution can be strictly distinguished by hydrological characteristics (Figures 4 and 5). On the contrary, according to the results obtained in this study, phytoplankton species composition and abundance tend to change gradually along the cross-section, resulting in some transition zones between different hydrological characteristics. For example, from the Kuroshio area to the transition area, nutrient conditions gradually changed to oligotrophic conditions, and correspondingly, the phytoplankton abundance gradually decreased [31]. The composition and abundance of phytoplankton community also changed spatially. Although some mesoscale vortexes and secondary mesoscale gyres may cause instability in local water bodies, this spatial distribution of diatoms occurs when nutrient gradients are kept changing along latitudes for a certain period. However, phytoplankton gradual adaptation to oligotrophic conditions depends on the species composition of diatoms and dinoflagellates [32–34].

In addition to changes in phytoplankton abundance between different hydrological characteristics, variations in diatoms and dinoflagellates abundance within the same hydrological characteristics were also found (Figures 4 and 5), suggesting that mesoscale circulation could play an important role in phytoplankton distribution [35]. Due to their poor activity and high potential growth rate, diatoms can reproduce rapidly in circulation and in water with high nutrient content. However, the disadvantage of poor mobility comes with its advantage. The circulation can not only bring new nutrient supplements, but also enable diatoms to distribute evenly in the sea area with strong circulation [36]. This also explains the high diatom abundance in Group A under the influence of NGCC. In fact, dinoflagellates are more susceptible to circulations and vortices, and the more violent the circulations and vortices are, the more their growth is inhibited [37]. The effects of circulations and vortices on dinoflagellates include inhibition of cell division, destruction of cell morphology, and inhibition of nutrient transport [38]. The characteristics of high temperature, high salinity, and high flow rate in the Kuroshio area exactly inhibited the abundance of dinoflagellates in this area, which was consistent with the previous research results [39].

4.2. Distribution of Trichodesmium

In the present study, *Trichodesmium* was the dominant cyanobacteria species. Marine *Trichodesmium* has been considered the most critical autotrophic nitrogen-fixing cyanobacteria since the 1960s [40]. *Trichodesmium* can be divided into two forms: clusters and free filaments. *Trichodesmium* is suitable for living in waters above 20 °C and has a special cellular air sac structure that allows it to move vertically within the upper 100 m of the ocean water column [41]. In the process of water bloom formation by *Trichodesmium*, a large amount of nitrogen is often fixed in a relatively short period of time. Therefore, the study of the nitrogen fixation rate of *Trichodesmium* is crucial for estimating the rate of nitrogen fixation in the ocean [42]. *Trichodesmium* is an important nitrogen-fixing organism in the ocean and a major contributor to the new productivity of the oligotrophic sea area [43]. The abundance of *Trichodesmium* in the tropical oligotrophic sea area is an issue of great concern [44].

In this study, cyanobacteria bloom was observed near New Guinea. The discovery of high abundance of *Trichodesmium* near the coast is consistent with the results of Campbell [45]. However, until now, it has not been clear how environmental factors control the latitude distribution of *Trichodesmium*. According to our results, temperature has an impact on the spatial distribution of *Trichodesmium*, which is similar to previous observations of tropical and subtropical oceans [46,47]. The optimum temperature for the growth and nitrogen fixation of *Trichodesmium* was between 20 °C and 30 °C. Our results show that there was a positive correlation between temperature and *Trichodesmium* abundance (Figure 6).

At present, there have been reports on the abundances of other oligotrophic salts in the oceanic region: Bonnet found that *Trichodesmium* has the highest abundance of trichomes L^{-1} (1.85) in the equatorial WPO [48]; Zhang [49] found that the average abundances of *Trichodesmium* in the central, eastern, and southern Indian Ocean were 1.76, 0.87 and 1.52, respectively. Therefore, this study investigates the high abundance of *Trichodesmium*, which is consistent with previous studies. Previous studies have not clarified which factors are the main causes of *Trichodesmium* growth (possibly temperature, wind, iron, phosphorus, etc.) [50,51]. Many researchers believe that temperature is the most important factor affecting the growth of *Trichodesmium* [52]. However, we believe that there is no single positive correlation between temperature and *Trichodesmium* growth, which is consistent with the study by Chang [50]. In the tropical WPO, where the temperature was not restricted, Group A had the highest temperature, but the abundance of *Trichodesmium* in Group A was not the highest. The highest value of *Trichodesmium* was in Group C, which had the second-highest temperature (Table 3, Figure 5). The cluster analysis divided the five groups according to the abundance of phytoplankton, which was consistent with the currents (Figure 3). We believe that marine physical processes such as circulation and hydrological characteristics have a profound impact on the spatial distribution of phytoplankton in the WPO.

4.3. Dominant Species and Their Preferred Environmental Factors

The conditions suitable for phytoplankton are often different from one community to another and even from one species to another. Comparing the dominant phytoplankton species of five groups, we conclude that *P. leniculatum* was the dominant species in the study area. *P. leniculatum* belongs to Dinophyta, and it is widely distributed in the world, including the Pacific Ocean, the Indian Ocean, the waters near Madagascar, and the Andaman Sea [53]. In the study area, the abundance of *P. leniculatum* in Group B was the lowest, which was affected by STCC, and it had the lowest average nutrient concentration. CCA analysis showed that *P. leniculatum* in Group B had a positive correlation with nitrate and silicate. Different from others, *C. kofoidii* was distributed evenly and had a high abundance in the whole study area. *C. kofoidii* reached the highest abundance in Group B, which was critically affected by Pacific Subtropical gyre. Atmospheric nitrogen fixation in the ocean is an important source of new nitrogen in the surface waters, which stimulates phytoplankton productivity and provides fuel for biological pumps. *Trichodesmium* is the main group responsible for marine nitrogen fixation in tropical waters [42]. The *R. intracellularis* has been shown to provide significant nitrogen input to the ocean on a regional scale [54]. The results of this study show that *R. intracellularis* was not observed in the equatorial region, while there was a high abundance in the region of transitional zone and the Kuroshio region. CCA analysis showed that *R. intracellularis* prefers to bloom in areas with higher nitrate and silicate.

5. Conclusions

This study investigated phytoplankton community structure in the WPO in 2017 and revealed the spatial variability of phytoplankton in community composition and abundance, as well as their relationship with physical ocean processes and environmental factors. A total of 332 species of phytoplankton were identified in this survey. The highest abundance of phytoplankton was found in the NECC and equatorial regions. *Trichodesmium* was widely distributed in the study area and reached the peak in WPWP, dinoflagellates were mainly affected by temperature, and diatoms were significantly correlated with nutrients (phosphate, nitrate, silicate, and nitrite). Phytoplankton were divided into five groups by cluster analysis, and the distribution of different groups was related to circulation and hydrological characteristics. These results show that physical ocean processes such as circulation and hydrological characteristics have a profound influence on the spatial distribution of phytoplankton. Different currents divide phytoplankton into different groups in space. In this investigation, we found that not only temperature and nutrient salinity, but also currents and water mass movements, affect the distribution of phytoplankton communities in the WPO. Despite the baseline data and information provided by this study, the phytoplankton of the WPO remain a mystery to us, especially the distribution of phytoplankton throughout the water column and eddies. Therefore, more long-term community studies are needed to further explore the role of phytoplankton in the marine biogeochemistry of the WPO.

Author Contributions: Conceptualization, J.S.; Data curation, Z.C.; Formal analysis, Z.C.; Funding acquisition, J.S.; Investigation, Z.C. and D.C.; Resources, D.C., S.W., H.Y., H.C., M.W. and J.S.; Supervision, J.S.; Writing—original draft, Z.C.; Writing—review and editing, J.S. All authors have read and agreed to the published version of the manuscript.

Funding: This research was supported by the National Key Research and Development Project of China (2019YFC1407805), the National Natural Science Foundation of China (41876134, 41676112, and 41276124), the Tianjin 131 Innovation Team Program (20180314), and the Changjiang Scholar Program of Chinese Ministry of Education (T2014253) through grants to Jun Sun.

Institutional Review Board Statement: Not applicable.

Data Availability Statement: All data are available from the authors upon request.

Acknowledgments: We thank all the members of Dongfanghong 2 for supporting and securing our scientific investigation on this cruise. Thanks to the CTD data provided by Jiwei Tian 's team at Ocean University of China.

Conflicts of Interest: The authors declare no conflict of interest.

References

1. Sun, J. Marine phytoplankton and biological carbon sink. *Acta Ecol. Sin.* **2011**, *31*, 5372–5378.
2. Wang, Y.; Kang, J.; Ye, Y.; Lin, G.; Yang, Q.; Lin, M. Phytoplankton community and environmental correlates in a coastal upwelling zone along western Taiwan Strait. *J. Mar. Syst.* **2016**, *154*, 252–263. [CrossRef]
3. Ahmed, A.; Kurian, S.; Gauns, M.; Chndrasekhararao, A.V.; Mulla, A.; Naik, B.; Naik, H.; Naqvi, S.W.A. Spatial variability in phytoplankton community structure along the eastern Arabian Sea during the onset of south-west monsoon. *Cont. Shelf Res.* **2016**, *119*, 30–39. [CrossRef]
4. Okazaki, Y.; Nakata, H.; Kimura, S. Effects of frontal eddies on the distribution and food availability of anchovy larvae in the Kuroshio Extension. *Mar. Freshw. Res.* **2002**, *53*, 403. [CrossRef]
5. Moita, M.T.; Pazos, Y.; Rocha, C.; Nolasco, R.; Oliveira, P.B. Toward predicting Dinophysis blooms off NW Iberia: A decade of events. *Harmful Algae* **2016**, *53*, 17–32. [CrossRef]
6. Wang, F.; Zhang, P.; Hu, D.X.; Seidel, H. Tropical Western Pacific circulation and seasonal changes. *Sci. Bull.* **2001**, *46*, 1998–2002. [CrossRef]
7. Gordon, A.L.; Fine, R.A. Pathways of water between the Pacific and Indian oceans in the Indonesian seas. *Nature* **1996**, *379*, 146–149. [CrossRef]
8. Yan, X.H.; Ho, C.R.; Zheng, Q.; Klemas, V. Temperature and size variabilities of the Western Pacific Warm Pool. *Science* **1992**, *258*, 1643–1645. [CrossRef]
9. Kawarada, Y. Distribution of plankton in the waters neighboring Japan in 1966 (CSK). *Oceanogr. Mag.* **1968**, *20*, 187–212.
10. Shiro, F. *Illustrations of the Kuroshio-Waters*; Chang Qi Publishing Culture Association: Hunan, China, 1990; pp. 1–170.
11. Sun, J.; Liu, D.Y.; Qian, S.B. Planktonic diatoms in the Ryukyu Islands and adjacent waters-species composition and abundance distribution in summer 1997. In *Chinese Oceanographic Anthology (II)*; Ocean University of China: Qingdao, China, 2000; pp. 170–182. (In Chinese)
12. Liu, D.Y.; Sun, J.; Qian, S.B. Planktonic dinoflagellates in the Ryukyu Islands and adjacent waters-species composition and abundance distribution in summer 1997. In *Chinese Oceanographic Anthology (II)*; Ocean University of China: Qingdao, China, 2000; pp. 158–169. (In Chinese)
13. Chen, Y.; Sun, X.; Zhu, M.; Zheng, S.; Yuan, Y.; Denis, M. Spatial variability of phytoplankton in the Pacific western boundary currents during summer 2014. *Mar. Freshw. Res.* **2017**, *68*, 1887–1900. [CrossRef]
14. Chen, Z.; Sun, J.; Zhang, G.C. Netz-phytoplankton community structure of the tropical Western Pacific Ocean in summer 2016. *Mar. Sci.* **2018**, *42*, 114–130. (In Chinese) [CrossRef]
15. Sun, J.; Liu, D.Y. A quantative research and analysis method for marine phytoplankton: An introduction to Utermöhl method and Its modification. *Adv. Mar. Sci.* **2002**, *20*, 105–112. [CrossRef]
16. Jin, D.X.; Chen, J.H. *Chinese Marine Planktonic Diatoms*; Shanghai Scientific & Technical Press: Shanghai, China, 1965; pp. 1–230.
17. Isamu, Y. *Illustrations of the Marine Plankton of Japan*; Hoikusha Press: Tokyo, Japan, 1991; pp. 1–158.
18. Sun, J.; Liu, D.Y. The Preliminary Notion on Nomenclature of Common Phytoplankton in China Sea Waters. *Oceanol. Limnol. Sin.* **2002**, *33*, 271–286. [CrossRef]
19. Ehrhardt, M.A.; Kremling, K.; Almgren, T.; Grasshoff, K.M. Methods of seawater analysis. *Chemie* **1976**. [CrossRef]
20. Dai, M.; Wang, L.; Guo, X.; Zhai, W.; Li, Q.; He, B.; Kao, S.J. Nitrification and inorganic nitrogen distribution in a large perturbed river/estuarine system: The Pearl River estuary, China. *Biogeosciences* **2008**, *5*, 1227–1244. [CrossRef]
21. Lorenzen, C.J. A method for the continuous measurement of in vivo chlorophyll concentration. *Deep-Sea Res. Oceanogr. Abstr.* **1966**, *13*, 223–227. [CrossRef]
22. Hu, D.X.; Wu, L.X.; Cai, W.J.; Gupta, A.S.; Ganachaud, A.; Qiu, B.; Gordon, A.L.; Lin, X.P.; Chen, Z.H.; Shijian Hu, S.J.; et al. Pacific western boundary currents and their roles in climate. *Nature* **2015**, *522*, 299–308. [CrossRef]
23. Lukas, R.; Firing, E.; Hacker, P.; Richardson, P.L.; Collins, C.A.; Fine, R.; Gammon, R. Observations of the Mindanao Current during the western equatorial Pacific Ocean circulation study. *J. Geophys. Res. Oceans* **1991**, *96*, 7089–7104. [CrossRef]
24. Zhu, J.; Zheng, Q.N.; Hu, J.Y.; Lin, H.Y.; Chen, D.W.; Chen, Z.Z.; Sun, Z.Y.; Li, L.Y.; Kong, H. Classification and 3-D distribution of upper layer water masses in the northern South China Sea. *Acta Oceanol. Sin.* **2019**, *38*, 126–135. [CrossRef]
25. Oksanen, J.F.; Blanchet, F.G.; Friendly, M.; Kindt, R.; Legendre, P.; McGlinn, D.; Minchin, P.R.; O' Hara, R.B.; Simpson, G.L.; Solymos, P.; et al. Vegan: Community Ecology Package. Available online: https://cran.r-project.org/web/packages/vegan/index.html (accessed on 20 August 2021).
26. Cravatte, S.; Delcroix, T.; Zhang, D.; Mcphaden, M.; Leloup, J. Observed freshening and warming of the western Pacific Warm Pool. *Clim. Dyn.* **2009**, *33*, 565–589. [CrossRef]
27. Kitajima, S.; Furuya, K.; Hashihama, F.; Takeda, S.; Kanda, J. Latitudinal distribution of diazotrophs and their nitrogen fixation in the tropical and subtropical western North Pacific. *Limnol. Oceanogr.* **2009**, *54*, 537–547. [CrossRef]

28. Sekine, Y.; Miyamoto, S. Influence of Kuroshio Flow on the Horizontal Distribution of North Pacific Intermediate Water in the Shikoku Basin. *J. Oceanogr.* **2002**, *58*, 611–616. [CrossRef]
29. Xie, L.; Tian, J.; Hu, D.X.; Wang, F. A quasi-synoptic interpretation of water mass distribution and circulation in the western North Pacific II: Circulation. *Chin. J. Oceanol. Limnol.* **2009**, *27*, 630–639. [CrossRef]
30. Lukas, R.; Lindstrom, E. The mixed layer of the western equatorial Pacific Ocean. *J. Geophys. Res. Oceans* **1991**, *96*, 3343. [CrossRef]
31. Mathias, G.; Hisayuki, A.; Fuminori, H. Phosphorus stress of microphytoplankton community in the western subtropical North Pacific. *J. Plankton Res.* **2013**, *35*, 146–157. [CrossRef]
32. Jeong, H.J.; Yoo, T.D.; Kim, J.S.; Seong, K.A.; Kang, N.S.; Kim, T.H. Growth, feeding and ecological roles of the mixotrophic and heterotrophic dinoflagellates in marine planktonic food webs. *Ocean Sci. J.* **2010**, *45*, 65–91. [CrossRef]
33. Greta, B.; Fabio, R.J.V.; Alberto, A.; Eric, P.; Pierella, K.; Ferrante, M.I.; Patrick, W.; Alessandra, R.; Chris, B.; Remo, S.; et al. Meta-omics reveals genetic flexibility of diatom nitrogen transporters in response to environmental changes. *Mol. Biol. Evol.* **2019**, *11*, 2522–2535. [CrossRef]
34. Luigi, C.; Quentin, C.; Damien, E.; Amos, K.; Eric, P.; Juan, J.P.K.; Fabio, R.J.V.; Emilie, V.; Samuel, C.; Shruti, M.; et al. Community-Level Responses to Iron Availability in Open Ocean Plankton Ecosystems. *Glob. Biogeochem. Cycles* **2019**, *33*, 391–419. [CrossRef]
35. Girault, M.; Arakawa, H.; Barani, A.; Ceccaldi, H.J.; Gregori, G. Distribution of ultraphytoplankton in the western part of the North Pacific subtropical gyre during a strong La Niña condition: Relations with the hydrological conditions. *Biogeosciences* **2013**, *10*, 5947–5965. [CrossRef]
36. Estrada, M.; Berdalet, E. Phytoplankton in a turbulent world. *Sci. Mar.* **1997**, *61*, 125–140. [CrossRef]
37. Thomas, W.H.; Gibson, C.H. Quantified small-scale turbulence inhibits a red tide dinoflagellate, Gonyaulax polyedra Stein. *Deep. Sea Res. Part. A Oceanogr. Res. Pap.* **1990**, *37*, 1583–1593. [CrossRef]
38. Smayda, T.J. Harmful algal blooms: Their ecophysiology and general relevance to phytoplankton blooms in the sea. *Limnol. Oceanogr.* **1997**, *42*, 1137–1153. [CrossRef]
39. Sullivan, J.M.; Swift, E.; Donaghay, P.L.; Rines, J.E.B. Small-scale turbulence affects the division rate and morphology of two red-tide dinoflagellates. *Harmful Algae* **2003**, *2*, 183–199. [CrossRef]
40. Dugdale, R.C.; Menzel, D.W.; Ryther, J.H. Nitrogen fixation in the Sargasso Sea. *Deep Sea Res.* **1961**, *7*, 297–300. [CrossRef]
41. Laroche, J.; Breitbarth, E. Importance of the diazotrophs as a source of new nitrogen in the ocean. *J. Sea Res.* **2005**, *53*, 67–91. [CrossRef]
42. Karl, D.; Michaels, A.; Bergman, B.; Capone, D.; Carpenter, E.; Letelier, R.; Lipschultz, F.; Paerl, H.; Sigman, D.; Stal, L. Dinitrogen fixation in the world's oceans. *Biogeochemistry* **2002**, *57–58*, 47–98. [CrossRef]
43. Toby, T.; Emilio, M.; Poulton, A.J.; Bowie, A.R.; Harbour, D.S.; Woodward, E.M.S. Large-scale latitudinal distribution of Trichodesmium spp. in the Atlantic Ocean. *J. Plankton Res.* **2003**, *58*, 405–416. [CrossRef]
44. Capone, D.G.; Zehr, J.P.; Paerl, H.W.; Bergman, B.; Carpenter, E.J. Trichodesmium, a Globally Significant Marine Cyanobacterium. *Science* **1997**, *276*, 1221–1229. [CrossRef]
45. Campbell, L.; Carpenter, E.J.; Montoya, J.P.; Kustka, A.B.; Capone, D.G. Picoplankton community structure within and outside a Trichodesmium bloom in the southwestern Pacific Ocean. *Vie Milieu* **2005**, *55*, 185–195.
46. Stal, L.J.; Severin, I.; Bolhuis, H. *The Ecology of Nitrogen Fixation in Cyanobacterial Mats*; Springer: New York, NY, USA, 2010; Volume 675, pp. 31–45. [CrossRef]
47. Zehr, J.P.; Ward, B.B. Nitrogen Cycling in the Ocean: New Perspectives on Processes and Paradigms. *Appl. Environ. Microbiol.* **2002**, *68*, 1015–1024. [CrossRef]
48. Bonnet, S.; Biegala, I.C.; Dutrieux, P.; Slemons, L.O.; Capone, D.G. Nitrogen fixation in the western equatorial Pacific: Rates, diazotrophic cyanobacterial size class distribution, and biogeochemical significance. *Glob. Biogeochem. Cycles* **2009**, *23*, 45–62. [CrossRef]
49. Zhang, D.S.; Wang, C.S.; Wang, X.G.; Liu, Z.S.; Gao, X.H. The large-scale distribution of Trichodesmium in the tropical and subtropical Pacific Ocean and the southern Indian Ocean. *Acta Oceanol. Sin.* **2010**, *32*, 148–154. [CrossRef]
50. Chang, J.; Chiang, K.P.; Gong, G.C. Seasonal variation and cross-shelf distribution of the nitrogen-fixing cyanobacterium, Trichodesmium, in southern East China Sea. *Cont. Shelf Res.* **2000**, *20*, 479–492. [CrossRef]
51. Karl, D.M.; Tien, G. Temporal variability in dissolved phosphorus concentrations in the subtropical North Pacific Ocean. *Mar. Chem.* **1997**, *56*, 77–96. [CrossRef]
52. Capone, D.; Carpente, E. Nitrogen fixation by marine cyanobacteria: Historical and global perspectives. *Bull. Linstitut Océanogr.* **1999**, *19*, 235–256.
53. Polat, S.; Koray, T. Planktonic dinoflagellates of the northern Levantine Basin, northeastern Mediterranean Sea. *Eur. J. Protistol.* **2007**, *43*, 193–204. [CrossRef] [PubMed]
54. Carpenter, E.J.; Montoya, J.P.; Burns, J.A.; Mulholland, M.R.; Capone, D.G. Extensive bloom of a N2-fixing diatom/cyanobacterial association in the Tropical Atlantic Ocean. *Mar. Ecol. Prog. Ser.* **1999**, *185*, 273–283. [CrossRef]